

**Inverse vulcanized conductive polymer for Li-S battery cathode**

Journal:	<i>Journal of Materials Chemistry A</i>
Manuscript ID	TA-ART-07-2020-006537.R1
Article Type:	Paper
Date Submitted by the Author:	29-Aug-2020
Complete List of Authors:	Gao, Guoping; Lawrence Berkeley National Laboratory, Berkeley, Sun, Xiaotian; Luoyang Normal University Wang, Lin-Wang; Lawrence Berkeley National Laboratory,

Inverse vulcanized conductive polymer for Li-S battery cathode

Guoping Gao¹, Xiaotian Sun^{1,2}, Lin-Wang Wang^{1*}

1. Materials Sciences Division, Lawrence Berkeley National Laboratory, Berkeley, California 94720, USA. E-mail: lwawang@lbl.gov
2. College of Chemistry and Chemical Engineering, and Henan Key Laboratory of Function-Oriented Porous Materials, Luoyang Normal University, Luoyang 471934, P. R. China

Abstract

Polymers with a broad range of properties, structural diversity, and mechanical flexibility, have been adopted in all aspects of Li-S batteries. However, currently explored polymers for Li-S cathode suffer from low conductivity, low S content, and poor cycling performance. In the first principle study, we theoretically design a new class polymer, poly (2-vinyl, 1, 4-phenylene sulfide), by modifying the conductive poly (1, 4-phenylene sulfide) via vinyl to enhance its ability to vulcanize with element S. We compare the properties of the experimentally realized sulfur vulcanized polymers via condensation and our designed sulfur vulcanized polymers via crosslinking as Li-S battery cathode, in terms of gravimetric and specific capacities, as well as structural stability during the lithiation. Overall, we find our designed polymer possesses better conductivity, higher specific capacity and gravimetric energy densities, better kinetic stability, and restricts the shuttle effect more efficiently than the current experimentally explored one. Also, the cross-linked sulfur compounds can be activated efficiently due to the short transport lengths rather than dissolution in the electrolyte during battery operation. Therefore, we believe our designed polymer cathode is promising for practical applications.

Introduction

Getting rid of fossil fuels and achieving the net-zero carbon emission urge us to explore and develop sustainable energy sources and technologies. However, the generation of renewable energy like solar and wind is intermittent. The energy storage system based on the battery is a vital technology to stabilize the renewable energy access and enhance energy security¹. On the other hand, batteries are an integrated part of cell phones, laptop computers, and electric vehicles². Lithium-sulfur (Li-S) batteries, using the earth-abundant sulfur as the cathode, are considered as the next generation batteries beyond lithium-ion batteries due to their high theoretical energy density (2567 Wh/kg) and lower cost³⁻⁵. However, there are several main challenging restrict their commercial potential: 1) the insulation of elemental sulfur and final discharge products (Li_2S_n , $n=1-2$) impedes the lithiation process; 2) the shuttle effect of dissolvable intermediates (Li_2S_n , $n=4-8$) reduces the active materials and causes short circuit effects; 3) the volumetric shrinkage/expansion among the sulfur (density of 2.07 g/cm³) and product Li_2S (density of 1.66 g/cm³) occurring on the cathode during the charge/discharge processes induces the cathode deformation.

Polymers with a broad range of properties, structural diversity, and mechanical flexibility, have

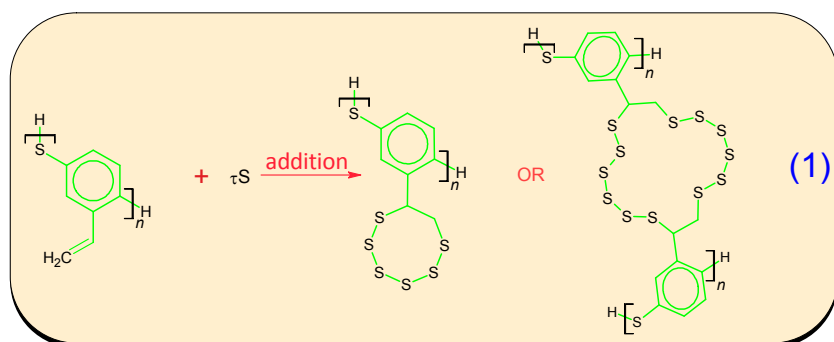
been adopted in almost all aspects of Li-S batteries, such as cathode, separator, electrolyte, anode, and interlayer⁶. Buffering the volume change efficiently and resisting polysulfides shuttling are the most well-known benefits of polymers due to their mechanical flexibility and side group chemical binding adjustability. Furthermore, various advanced polymers with unique structures and properties have been designed via tailoring the functional groups for particular applications in Li-S batteries. Polar polymers, such as poly(vinylidene fluoride-hexafluoropropylene)⁷, carboxymethyl cellulose-butadiene styrene rubber⁸, gum arabic⁹, are selected as binders in Li-S systems to link conductive carbon, insulated sulfur, and current collector. Uniformly dispersing these composites can suppress the shuttle effects of polysulfides and achieve ion/electron conductivity simultaneously. The conjugated polymers are selected as conductive binders to facilitate binding between charge/ionic conducting materials with the electro-active materials¹⁰. Sulfur-containing polymers, usually with S-S bonds, have been explored as electro-active materials for Li-S batteries based on the electrochemically-reversible transformation¹¹. However, the sulfur content in these polymers is relatively low. A more promising approach is to copolymerize, or inverse vulcanize element S onto the conductive backbone polymer¹²⁻¹⁴, which can not only increase the sulfur content, but also maintain the good conductivity.

Conductive polymers (CPs) are a class of organic materials with unique electrical and optical properties similar to those of inorganic semiconductors and metals.¹⁵ They can be readily assembled into different parts of Li-S batteries with multifunctional applications by using simple electropolymerization processes.^{10, 14, 16} However, the conductive polymers containing conjugated aromatic rings are often more rigid, and less flexible to deal with, and its modification with S has not been fully investigated. Besides, the theoretical research on the underlying mechanism in this area is rare. One challenge is that such a battery system can be complex, and not easy to study using straightforward *ab initio* methods¹⁷. In this first-principle work, we modify the conductive poly (1, 4-phenylene sulfide) via vinyl to enhance its ability to vulcanize with element S inversely. During the vulcanization, we find the crosslinking is the main reaction while the cycloaddition is the side reaction for the designed polymer. In the following, the properties of the current experimental realized sulfur vulcanized polymers via condensation and our theoretically designed sulfur vulcanized polymers via crosslinking will be compared systematically as Li-S battery cathode. Based on this comparison, we found that the crosslinking polymer is superior to the experimentally realized condensation polymer in electric conductivity, energy capacities, and cycling performance.

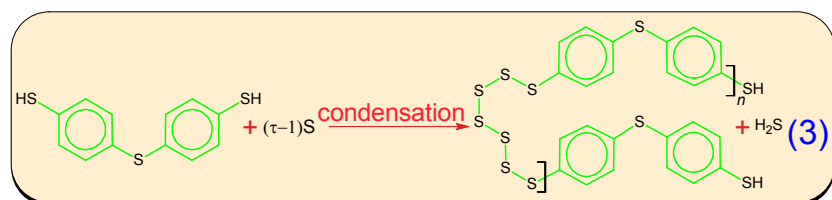
Computational detail

All calculations were performed using the planewave DFT method implemented in the PWmat code^{18, 19} with norm-conserving pseudopotential except the quantum transport calculations. The exchange-correlation interactions were treated by the generalized gradient approximation in the form of the Perdew–Burke–Ernzerhof functional^{20, 21}. The Van der Waals interaction was described by using the empirical correction in Grimme's scheme, i.e. DFT+D₂²². The electron wave functions were expanded by plane waves with cut-off energies of 680 eV, and the convergence tolerance for residual force and energy on each atom during structure relaxation were set to 0.005 eV Å⁻¹ and 10⁻⁵ eV, respectively.

The schematic of inverse vulcanization S into polymer via addition reactions and condensation reaction are summarized in formula (1) and (3) in Fig. 1, respectively. Here, we use S_τ^* in Fig. 1 to represent the polymer, and polymer with S_τ chains binding, respectively. The τ is the maximum S atoms in the chains. The n in Fig. 1 is the degree of polymerization. As we know, a polymer blend is between the amorphous form and quasi-one-dimension form, with its main backbone chain interacting with other chains via Van der Waals interaction. To simplify the simulation of the amorphous properties of the randomly oriented polymer, molecular models (the n is set to 3 and 1 for addition reaction and condensation reaction, respectively as shown in Fig. 2), which allows the polymer to adjust the orientations of active sites freely in chemical reactions, are used in DFT calculation to obtain the atom-level chemical properties, including the vulcanization energy, and Li binding energy. To estimate the macroscopic quantities, like the S content and energy capacity, we treat polymers as infinity one-dimension materials with repeating units (n is infinity, as shown in Fig. 5).



$$E_{vul} = E_{S_\tau^*} - \tau/8E_{S_8} - E_* \quad (2)$$

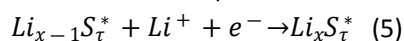


$$E_{vul} = E_{S_\tau^*} + nE_{H_2S} - n(\tau-1)/8E_{S_8} - (n+1)E_{monomer} \quad (4)$$

Figure 1 The schematic of inverse vulcanization S into polymer via addition reactions and condensation reaction

The formula for vulcanization energy of addition reaction and condensation reaction is shown as equation (2) and (4), respectively. The E_{S_8} is the average energy of S_8 in the solid-state phase. Except for E_{S_8} , all the other terms are calculated in an implicit solvent model with a dielectric constant of 7.8 to represent 1,2-dimethoxyethane(DME)/1,3-dioxolane(DOL) (V:V=1: 1)²³.

The elemental step of Xth Li-ion in the discharge process can be expressed by:



The voltage of reaction (5) generated can be obtained by:

$$U = - \frac{E_{Li_x S_\tau^*} - E_{Li_{x-1} S_\tau^*} - E_{Li^+}}{e} \quad (6)$$

It is a challenge to calculate the total energy of Li^+ (E_{Li^+}) directly. However, we can use the unit energy of Li in bulk ($E_{Li \text{ per atom in bulk}}$) to represent E_{Li^+} .

$$U (\text{verus } Li^+ / Li) = - \frac{E_{Li_x S_\tau^*} - E_{Li_{x-1} S_\tau^*} - E_{Li \text{ per atom in bulk}}}{e} \quad (7)$$

By do that, the voltage obtained is referenced to the potential of Li^+/Li equilibrium voltage. Therefore, we assumption Li atom, rather than Li-ion, is added to S_τ^* one by one during the lithiation procedure, which reduces the complexity of the simulation as well. In practice, the discharge process is a thermodynamics disequilibrium process under an external circuit with electrolyte involving. Under such a condition, the Li-ion may shuffle to any part of the cathode surface. In another word, the energy-favorable site is the probable position of Li-ion thermodynamically, but the only position in every step kinetically. To find the as favorable configuration of $Li_x S_\tau^*$ as possible, we consider 5 to 10 binding positions of the Li atoms around the LUMO of the $Li_{x-1} S_\tau^*$ for the initial screening as the s-level of Li atoms is likely to hybridize with the local empty state (in the local density of state), e.g., the LUMO level, to lower the total energy, and form some bond. The top three most stable $Li_x S_\tau^*$ configurations based on geometry relaxation are chosen to do the molecular dynamic calculation in the NVT ensemble at 350 K for 1.5 ps. The final molecular dynamic calculation configurations are relaxed further to obtain the most energy-favorable solution. The formation energy of the Xth Li in the discharge process is calculated as the following:

$$E_{Li_{xth}} = E_{Li_x S_\tau^*} - E_{Li_{x-1} S_\tau^*} - E_{Li \text{ per atom in bulk}} \quad (8)$$

Then, the total formation energy of $Li_x S_\tau^*$ is obtained by the following equation:

$$E_{Form} = \sum_{i=1}^x E_{Li_{xth}} \quad (9)$$

Here, the $E_{Li \text{ per atom in bulk}}$ is the energy per Li atom in its metallic bulk form. Based on Eq. (7) and (9), we can obtain the average discharge voltage via equation (10):

$$U_{ave} (\text{verus } Li^+ / Li) = \frac{\sum_{i=1}^x E_{Li_{xth}}}{x} \quad (10)$$

The gravimetric energy density is calculated by equation (11):

$$E_{\text{gravimetric energy density}} = E_{form}/m \quad (11)$$

Where, the m is the mass of total polymer Li charged cathode materials ($Li_x S_\tau^*$). The specific capacity is obtained by equation (12):

$$C = q/m \quad (12)$$

Here, q equals the quantity of Li consumed in the discharge process as one Li atom donated one electron.

Results and discussion

The sulfur in the original conjugated π polymer of poly (1, 4-phenylene sulfide) is relatively less and not active sites for Li-S battery. Inserting the S into the backbone through condensation polymerization will break the electronic connectivity of conjugated π bonds. To avoid these issues, the side chain is introduced on the backbone as the reactive sites for sulfur vulcanization. There are four hydrogen atoms per unit in the backbone of poly (1, 4-phenylene sulfide), which can be

replaced by substitutes to yield a well-designed structure for particular functions, e.g. to facilitate the sulfur vulcanization.

The unsaturated functional groups such as alkenes and allyls are the most common reactive sites for sulfur vulcanization. To screening out the suitable substitutes and approaches for sulfur vulcanization, the C=C bonds in the edge and middle of Decene are compared as the activity sites for vulcanization via crosslinking and cycloaddition, as shown in Fig. S1 and Tab. S1, supporting information. As for the vulcanization method, the crosslinking approach, rather than the cycloaddition approach, is most likely to graft the stable S_6^* chain on 5-Decene. In crosslinking sulfur vulcanization, the edge C=C bond in 1-Decene is thermodynamically more favorable than the C=C bond in the middle of the chain (5-Decene) for all ranges of the sulfur chain vulcanization due to the smaller steric effects as shown in Fig. S2. Vinyl group is the simplest S vulcanization sites with edge C=C bond and therefore is chosen as the substitute unit to be inserted in poly (1, 4-phenylene sulfide) as shown in Fig. 1. In the poly (2-vinyl, 1, 4-phenylene sulfide), the vinyl side chain is grafted onto the conjugated backbone. The designed polymer is expected to maintain the excellent electronic and mechanic properties of the backbone.

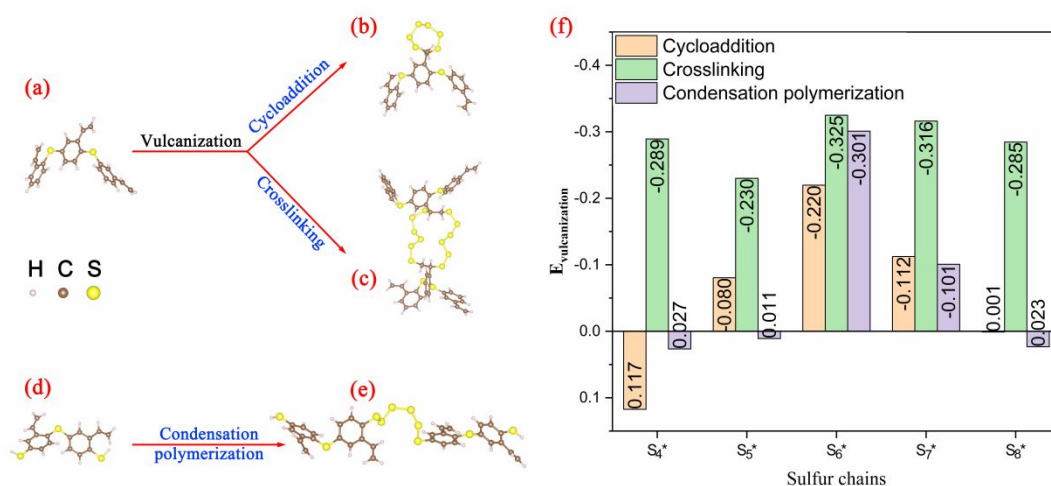


Figure 2 Vulcanization of S into the polymer via cycloaddition (b), crosslinking(c) and condensation (e); the vulcanization energies of different S chains via the above three approaches (f). For the comparison purpose, we used poly (2-vinyl, 1, 4-phenylene sulfide) in all the three different vulcanization ways.

In practice, the sulfur-rich polymer can be synthesized via the inverse vulcanization procedure suggested by Pyun *et al.*^{24, 25} The S_8 is melted at 185 ° C. Then, the polymer with unsaturated functional groups is added into orange molten sulfur via a syringe. The mixture is stirred for 8-10 minutes for the sulfur diradicals propagation on the unsaturated functional groups efficiently. The final product is chemically stable glassy copolymers. The reaction mechanism underneath is very complex and is out of our capability to mimic via DFT calculation. However, based on the analysis

of the product in the experiment, the sulfur is chemically combined between the long-chain polymer, mostly in the form of cross-links, or bridges. Thus, theoretically, we have chosen the main products well-known in the experiment as our computational subjects.

There are three different ways of vulcanization of S into the polymer as suggested in reference:^{24, 26} quenching of the radical sulfur chain ends with vinyl side chain through cycloaddition (hereinafter referred to as 'cycloaddition polymer', see Fig. 2b); or crosslinking (hereinafter referred to as 'crosslinking polymer', see Fig. 2c); and the condensation reaction between 2,3'-vinyl, 4,4'-thiobisbenzenethiol monomer and sulfur chain (hereinafter referred to as 'condensation polymer', see Fig. 2e). The cycloaddition and crosslinking approaches only modify the side chain of the polymer which may occur in the same reaction condition simultaneously. In contrast, in the condensation reaction, the S chain becomes a part of the backbone, which is a different approach requiring different precursor monomers.

The vulcanization energies of different S chains via the above three approaches are compared in Fig. 2f. As we can see, all these three approaches can chemically stabilize the high contents of sulfur in the polymer. In the addition reaction, the vulcanization energies of crosslinking are more negative than that of cycloaddition throughout the entire range of S chains, indicating that the crosslinking is the main reaction while the cycloaddition is the side reaction, which is consistent with results of 5-Decene in supporting information. The Boltzmann distribution based on the vulcanization energy indicates that the probability of vulcanization via crosslinking will be 97%. In comparison, the probability of cycloaddition is only 3% at the temperature of 185°C²⁵ (See Table S2 in the supporting information). Besides, the most stable S chains on the polymer are S₆* in all these three cases with a negative vulcanization energy of -0.220 eV, -0.325 eV, and -0.301 eV for cycloaddition, crosslinking and condensation reaction, respectively. It should note that it is still possible to synthesize other lengths, depending on the amount of S added during the synthesis process. It has been reported the average S chain length in such systems is about 5 calculated from the sulfur content in the experiment, only slightly shorter than ours²⁶. Therefore, only the crosslinking polymer and condensation polymer with S₆* are compared for the cathode design in Li-S batteries.

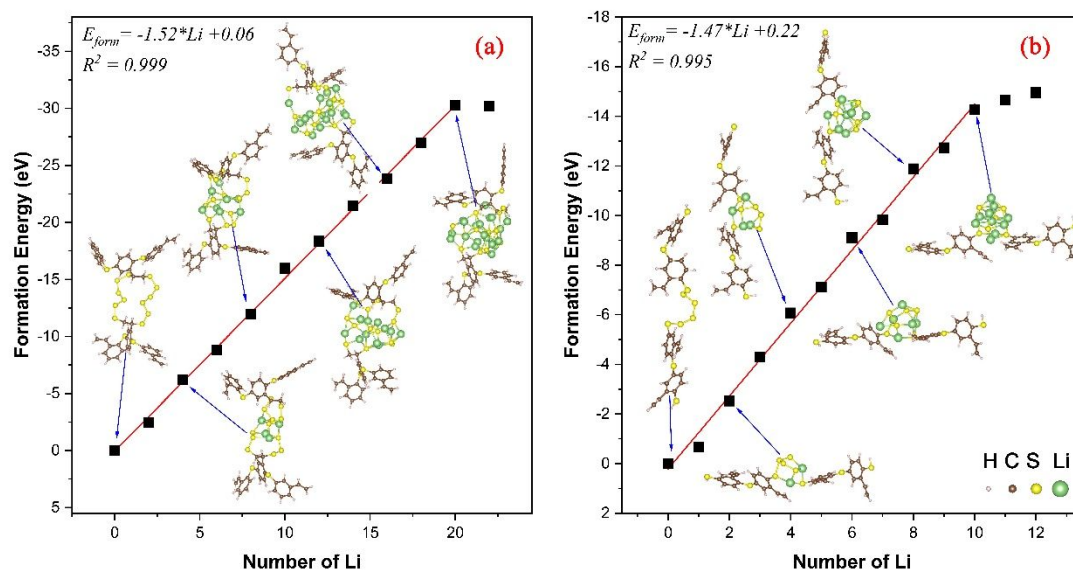


Figure 3 The formation energies of Li_xS_τ on crosslinking polymer (a) and condensation polymer (b) as a function of the number of Li in the solvent.

To simulate the discharge process in Li-S battery, the Li atom is added to S vulcanized polymer one Li at a time following the approach mentioned in the calculation details. The formation energies of Li_xS_τ on crosslinking polymer (Fig. 3a) and condensation polymer (Fig. 3b) as a function of the number of Li in the solvent is calculated, respectively via Eq. 9. Some intermediate configurations are shown as well to illustrate discharge processes. In both cases, the Li atoms attack the middle S atoms in the S chains that are not bound to carbon initially and then break down all the S-S bonds forming a Li_xS_τ cluster gradually. However, the strong covalent C-S bonds forming during the vulcanization binding the clusters and the frameworks of the polymers remain firmly throughout the whole discharge process, and they are never broken. The strong C-S bonds play an essential role in preventing sulfur from retaining during the discharge process. The previous computational studies on the sulfur/graphene model indicate that sulfur-carbon bonding prevents sulfur from retaining its stable cyclic structure before lithiation yielding a distribution of linear sulfur chains tightly bonded to the carbon backbone^{27, 28}.

Remarkable, the formation energies of Li_xS_τ are almost a linear function of the number of Li until they reach plateaus in both polymers. As we can see, the formation energy of the 21st Li in crosslinking polymer is positive, indicating that the process is thermodynamically favorable. In condensation polymer, the formation energies of 11th and 12th Li are still negative. However, the formation energies are significantly smaller than that of the previous Li. These small formation energies will significantly reduce the average discharge voltage based on Eq. 10 and the analysis in Fig. 5. Besides, the 11th Li, for example, is locating on the top of the benzene ring rather than embedded in the previous $\text{Li}_x\text{S}_\tau^*$ as shown in Fig. S3 in supporting information, which is expected to be dissolved in the electrolyte during battery operation. Therefore, to maintain the high discharge, and to be stable against the dissolution, the maximum Li number for crosslinking and condensation polymers is 20 and 10 respectively. Note that, the total S number (τ) involved in the crosslinking polymer and condensation polymer per unit is 12 and 6, respectively. The final clusters

in both cases can be expressed by $n(\text{Li}_{10}\text{S}_6)$. If we take out one S per two S-C bonds which are not involving the discharge process, the final cluster has a formula of Li_2S , the same as the ultimate reduced S for Li-S battery. Interestingly, for the conventional Li-S battery, Li_2S is an insulated crystal²⁹. Here, the $n(\text{Li}_{10}\text{S}_6)$ is a cluster. As the final product of inverse vulcanized polymer is chemically stable glassy copolymers²⁴, it is reasonable to use the amorphous $n(\text{Li}_{10}\text{S}_6)$ cluster to represent the lithiation product, which appeared in the previous work as well³⁰. All these lithiation behaviors are consistent in the experimental results of SPAN cathode³¹. In the SPAN cathode experiment, the sulfur atoms in the poly(sulfide)s chain, which are not bound to carbon but to other sulfur, are first released from the backbone to form the single discharge product of Li_2S .

The average discharge voltages versus Li^+/Li can be estimated by the slopes between the formation energy and the Li number (or the number of electron transfer) as shown in Eq. 10. The average discharge voltages of these two polymers are almost constants throughout the entire discharge process (1.52 V versus Li^+/Li for crosslinking polymer and 1.47 V versus Li^+/Li for condensation polymer as shown in Fig. 3). Different from the conventional elemental sulfur cathode, these polymer cathodes exhibit a unique redox process with only one discharge voltage plateau. This voltage discharge profile of our model is consistent with the experimental result of SPAN cathode³¹, in which only one shoulder is found in the discharge profile with a voltage of ~ 1.5 V versus Li^+/Li . Liu *et al.* also find the equilibrium voltage for the Li_2S Nano-sized cluster is 1.5 V versus Li^+/Li in their computational study³⁰. These voltages are about 0.7 eV lower than the equilibrium voltage of bulk Li_2S ⁵, due to the large specific surface area, the less coordinated Li and S atoms, and dangling bonds in the Li_2S clusters³⁰. It is interesting to note that if the Li_2S clusters stretch into a two-dimensional form, the discharge voltage can be increased to 1.74 V versus Li^+/Li in our previous work⁵.

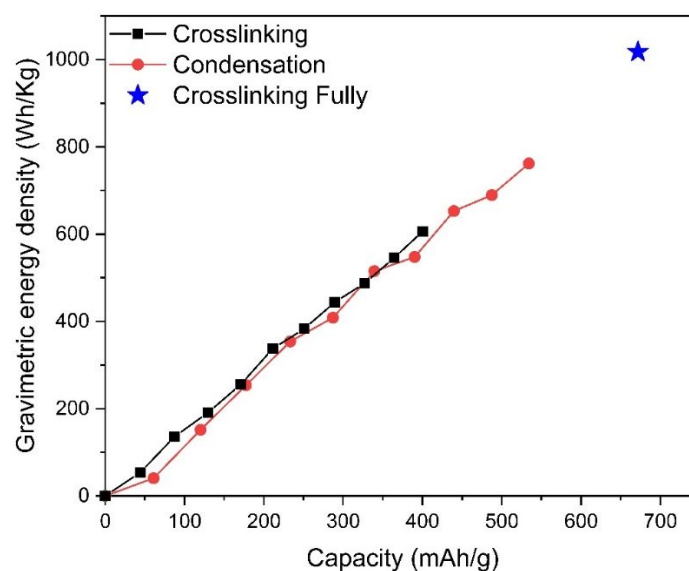


Figure 4 The gravimetric energy density between crosslinking polymers and condensation polymers as a function of the specific capacities in Li-S battery cathode.

The comparison of gravimetric energy densities of crosslinking polymers and condensation polymers as the cathode in Li-S battery is shown in Fig. 4. The maximum specific capacity for

condensation and crosslinking polymers are 534 mAh/g and 400 mAh/g, respectively. The corresponding gravimetric energy densities are 762 Wh/kg (condensation polymer) and 607 Wh/kg (crosslinking polymer). However, it should be noted that only 1/3 of Vinyl groups in our crosslinking polymer model are vulcanized, which results in a S content of only 49% in weight. If all the vinyl groups are vulcanized, the S mass content can reach 69% in weight, which is much higher than the value of condensation polymer (52%). The specific capacity and gravimetric energy densities for the fully vulcanized crosslinking polymer can be as high as 672 mAh/g and 1018 Wh/kg. Based on the experimental data of Polyphenyl polysulfide (PPPS-14)²⁶, the real specific capacity at 1 C rate is 61% of the theoretical specific capacity. We can estimate that the real specific capacity and gravimetric energy densities of designed polymer is about 413 mAh/g and 626 Wh/kg at 1 C rate, which is much higher than the state-of-the-art Li-S value obtained by OXIS Energy Ltd(450 Wh/kg)³².

The next question of utmost importance is the ability of these polymers to prevent the dissolution of Li-polysulfide. As shown in Fig. 3, the polymers capture the whole clusters, Li_xS_τ , firmly via strong covalent C-S bonds throughout the whole discharge process. This indicates the Li_xS_τ clusters adhere to the polymers. Whether some smaller $\text{Li}_2\text{S}_\gamma$ cluster ($\gamma = 4, 6, \text{ or } 8$, since they are highly soluble in the solvent), can be dissolved from the $\text{Li}_x\text{S}_\tau^*$ is a very important question. We consider this question from the thermodynamic ground. For this purpose, we first set the total energies of $\text{Li}_x\text{S}_\tau^*$ as zero. Due to the large numbers of possible systems and configurations, only the $\text{Li}_2\text{S}_{12}^*$ (LiS_6^*) and $\text{Li}_{10}\text{S}_{12}^*$ (Li_5S_6^*) and $\text{Li}_{20}\text{S}_{12}^*$ ($\text{Li}_{10}\text{S}_6^*$) are chosen to represent the initial, middle, and final discharge configurations in crosslinking polymer (condensation polymer) to study the dissolution stability. For condensation polymer, the dissolution energies of the breakaway lithium-polysulfides $\text{Li}_2\text{S}_\gamma$ from LiS_6^* are slightly negative at initial discharge state, -0.1 eV, -0.14 eV, and -0.17 eV for $\gamma = 4, 6, \text{ and } 8$ respectively, indicating that LiS_6^* is vulnerable to being dissolved into a shorter sulfur chain and smaller $\text{Li}_2\text{S}_\gamma$ cluster. As the lithiation process progresses further, Li_5S_6^* and $\text{Li}_{10}\text{S}_6^*$ become thermodynamically stable against the dissolution with positive dissolution energies. The dissolution problem for condensation polymer at the initial charge state may give rise to chain breaking after the electro-redox and lead to the loss of the active materials. This issue can be addressed in the crosslinking polymer. The dissolution energies in the crosslinking polymer case are all positive throughout the whole discharge process, thus thermodynamically stable. To check the kinetic stability further, the initial product of vulcanization of S via crosslinking and final lithiation product of crosslinking polymer with $\text{Li}_{20}\text{S}_{12}$ are used to carry out ab initio molecular dynamic simulations together with 1,2-dimethoxyethane(DME)/1,3-dioxolane(DOL) (mole ratio=1:1) explicit electrolyte in the NVT ensemble at 300 K for 3 ps. These final configurations are shown in Fig. S5, supporting information. As we can see, no chemical bonds are formed between solvent and vulcanization S in the initial product (Fig. S5a); even though there are some 1,2-dimethoxyethane(DME) molecules bind on the Li atoms of the Li-S cluster in the final product (Fig. S5b), the whole Li-S cluster is stable, firmly binding to the polymer through S-C bonds. These phenomena confirm the crosslinking polymers system will be kinetically stable rather than being dissolved in the electrolyte during the lithiation. Above all, the crosslinking polymer can restrict the shuttle effect in the whole discharge process and kinetically stable. It is thus expected to have better cycling stability than the experimentally tested condensation polymer.

Table 1 The dissolution energies of 0.5 Li_2S_y ($y=4, 6, 8$) from Li_xS_t^* . * is the crosslinking polymer or condensation polymer. The total energies of Li_xS_t^* are set to be zero. Here the $\text{Li}_2\text{S}_{12}^*$ (Li_6S_6^*) and $\text{Li}_{10}\text{S}_{12}^*$ (Li_5S_6^*) and $\text{Li}_{20}\text{S}_{12}^*$ ($\text{Li}_{10}\text{S}_6^*$) are chosen to represent the initial, middle, and final discharge states in crosslinking polymer (condensation polymer).

Crosslinking polymer				Condensation polymer			
$\text{Li}_2\text{S}_{12}^*$	$\text{LiS}_8^* + \frac{1}{2}\text{Li}_2\text{S}_8$	$\text{LiS}_9^* + \frac{1}{2}\text{Li}_2\text{S}_6$	$\text{LiS}_{10}^* + \frac{1}{2}\text{Li}_2\text{S}_4$	LiS_6^*	$\text{S}_2^* + \frac{1}{2}\text{Li}_2\text{S}_8$	$\text{S}_3^* + \frac{1}{2}\text{Li}_2\text{S}_6$	$\text{S}_4^* + \frac{1}{2}\text{Li}_2\text{S}_4$
0	0.50	0.71	2.03	0	-0.17	-0.14	-0.10
$\text{Li}_{10}\text{S}_{12}^*$	$\text{Li}_9\text{S}_8^* + \frac{1}{2}\text{Li}_2\text{S}_8$	$\text{Li}_9\text{S}_9^* + \frac{1}{2}\text{Li}_2\text{S}_6$	$\text{Li}_9\text{S}_{10}^* + \frac{1}{2}\text{Li}_2\text{S}_4$	Li_5S_6^*	$\text{Li}_4\text{S}_2^* + \frac{1}{2}\text{Li}_2\text{S}_8$	$\text{Li}_4\text{S}_3^* + \frac{1}{2}\text{Li}_2\text{S}_6$	$\text{Li}_4\text{S}_4^* + \frac{1}{2}\text{Li}_2\text{S}_4$
0	2.41	1.72	1.46	0	3.40	0.63	0.19
$\text{Li}_{20}\text{S}_{12}^*$	$\text{Li}_{19}\text{S}_8^* + \frac{1}{2}\text{Li}_2\text{S}_8$	$\text{Li}_{19}\text{S}_9^* + \frac{1}{2}\text{Li}_2\text{S}_6$	$\text{Li}_{19}\text{S}_{10}^* + \frac{1}{2}\text{Li}_2\text{S}_4$	$\text{Li}_{10}\text{S}_6^*$	$\text{Li}_9\text{S}_2^* + \frac{1}{2}\text{Li}_2\text{S}_8$	$\text{Li}_9\text{S}_3^* + \frac{1}{2}\text{Li}_2\text{S}_6$	$\text{Li}_9\text{S}_4^* + \frac{1}{2}\text{Li}_2\text{S}_4$
0	11.09	6.54	3.13	0	13.65	9.69	5.86

Generally, the high solubility of polysulfides in the electrolyte plays an essential role to activate the insulated bulk sulfur and Li_2S but results in shuttle effects and S loss. Sparingly solvating electrolytes is a promising strategy for the challenge by optimizing and reducing the electrolytes under the framework of precipitation–dissolution mechanism³³⁻³⁵. We note that there are several ways to prevent dissolution. First, there is a report of a new electrolyte (hydrofluoroethers with bi-functional, amphiphilic surfactant-like design) which significantly reduces the polysulfide dissolution³⁶. Second, our theoretical calculations show Li_xS_y clusters anchored on the polymer can thermodynamically prevent such dissolution. We think combining the new electrolyte (which thermodynamically prevents the dissolution) and the stable binding of the Li_xS_y cluster to some anchoring site is likely to reduce the dissolution problem significantly. Given such a situation, the challenge is to activate the undissolved Li_xS_y . In a conventional setup, a big chunk (or large particle) is in contact with the electrode (e.g., Al substrate). Due to the limited electric conductivity, the reaction can only happen in the corner where the S atoms touch the electrode substrate. Thus, if the reaction produced Li_xS_y is not dissolved, due to the insulating nature of the Li_xS_y , the reaction will stop soon. To continue the reaction, we have to (1) expose the S or Li_xS_y to the electrolyte; (2) to have electron conductivity to the reaction site. For this, we think our nanocluster ($\sim 4.3\text{\AA}$ in radius) attached to the conductivity polymer can provide a solution. The small size of the nanocluster makes it always exposed to the liquid electrolyte; and the conductive polymer provides the electron conductivity needed to the reaction site. Therefore, the cross-linked sulfur compounds can be activated efficiently due to the short transport lengths rather than dissolution in the electrolyte during battery operation.

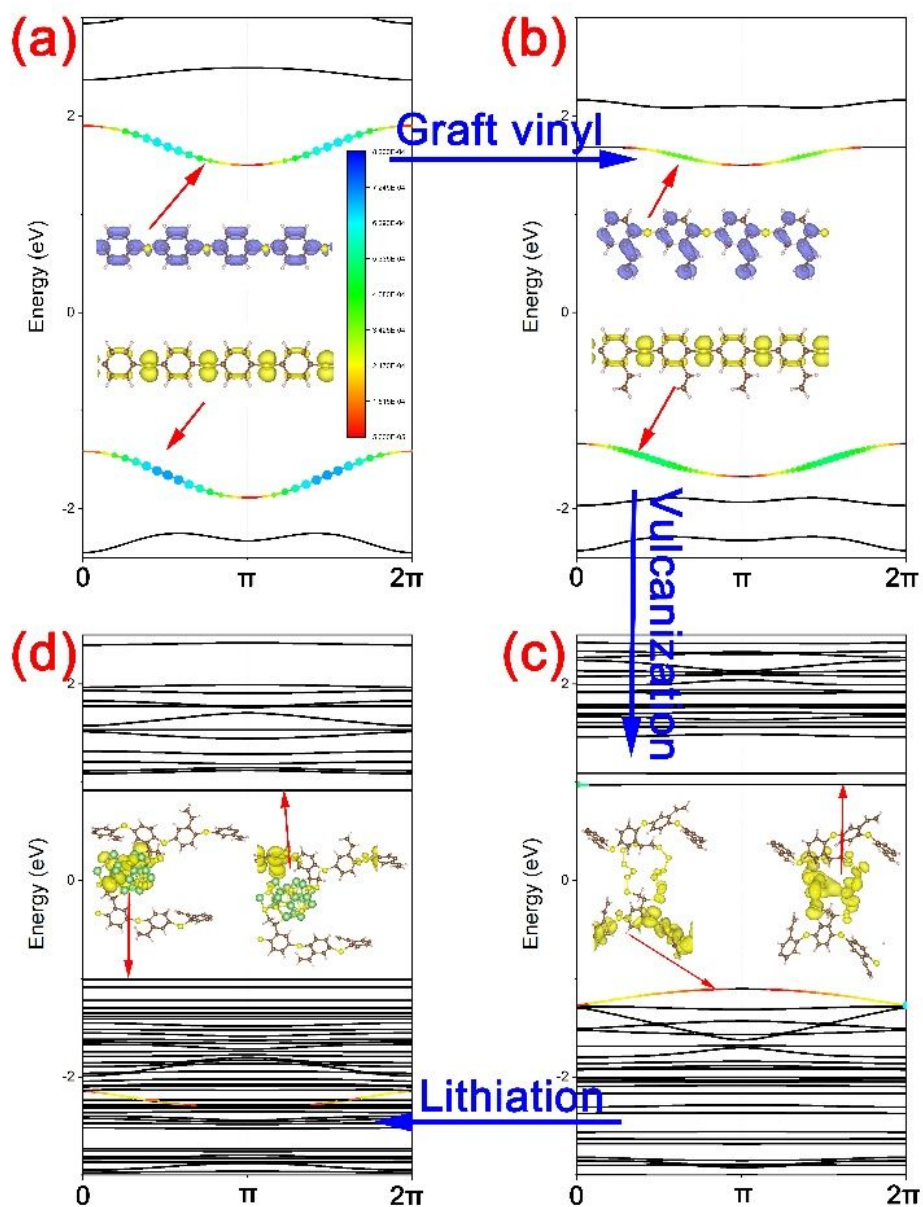


Figure 5 The evolution of band structures with group velocities of valence band maximum (VBM or HOMO) and the conduction band minimum (CBM or LUMO) of poly (1, 4-phenylene sulfide) (a), grafted with vinyl side chains (poly (2-vinyl, 1, 4-phenylene sulfide), b), vulcanization ($2S_6^*$, c), to lithiation ($Li_{20}S_{12}^*$, d). The color in the band structures indicates the weight of group velocities of VBM and CBM. The original VBM of backbone after lithiation is labeled with color too.

Electron conductivity is another critical issue for a good cathode in Li-S battery. The poly (1, 4-phenylene sulfide), with delocalized π -electron within the unsaturated backbone, can be converted to conductive polymers by appropriate oxidations or doping. Stronger electronic acceptors like (SbF_5 , AsF_5) can successfully enhance the p-type electronic conductivity of polyphenylene sulfide up to 2.7 S/cm.³⁷ The electronic properties can change after grafted vinyl, vulcanization, and lithiation. Fig. 5 presents the evolution of the band structure of the poly (1, 4-

phenylene sulfide) during these processes within the solvent. In poly (1, 4-phenylene sulfide) (Fig. 6a), the bandgap is as high as 2.92 eV. However, the HOMO and LUMO are delocalizing through the chain, which provides the ideal pathways for coherent charge transport. The bands of the vinyl group are far from the Fermi level. These two materials have similar energy dispersion near the band edge. The VBM and CBM are predominately contributed from the benzene ring and S atoms in the backbone. The group velocities of these two materials are similar ($\sim 7.0 \times 10^{-4}$ m/s for poly (1, 4-phenylene sulfide), while $\sim 5.0 \times 10^{-4}$ m/s for poly (2-vinyl, 1, 4-phenylene sulfide)). The similar group velocities confirm that the vinyl group has a small influence on the conductivity, and these two materials should be similar in the conductive properties. After vulcanization, the CBM is contributed from the S_6^* chains, while the VBM is still formed by benzene ring and S atoms in the backbone. The VBM is still delocalized, its group velocity ($\sim 2.7 \times 10^{-4}$ m/s) is only about 1/3 of that in poly (1, 4-phenylene sulfide) which decreases the conductivity of the polymer. It should be noted that this group velocity is much larger than that of vulcanization of S into the polymer via condensation ($\sim 1.5 \times 10^{-4}$ m/s, Fig. S4, supporting information). After lithiation, the electron donor Li will change the VBM via localized Li-S bonds, which decrease the group velocity further to 0. Therefore, the lithiation will deteriorate the conductivity of poly (2-vinyl, 1, 4-phenylene sulfide) gradually, or making it a hole polaron hopping like charge transport³⁰. Whether or not one can maintain a backbone band like transport will be a future challenge for design. One possibility is to have a narrower bandgap for the backbone, perhaps by side-chain manipulations.

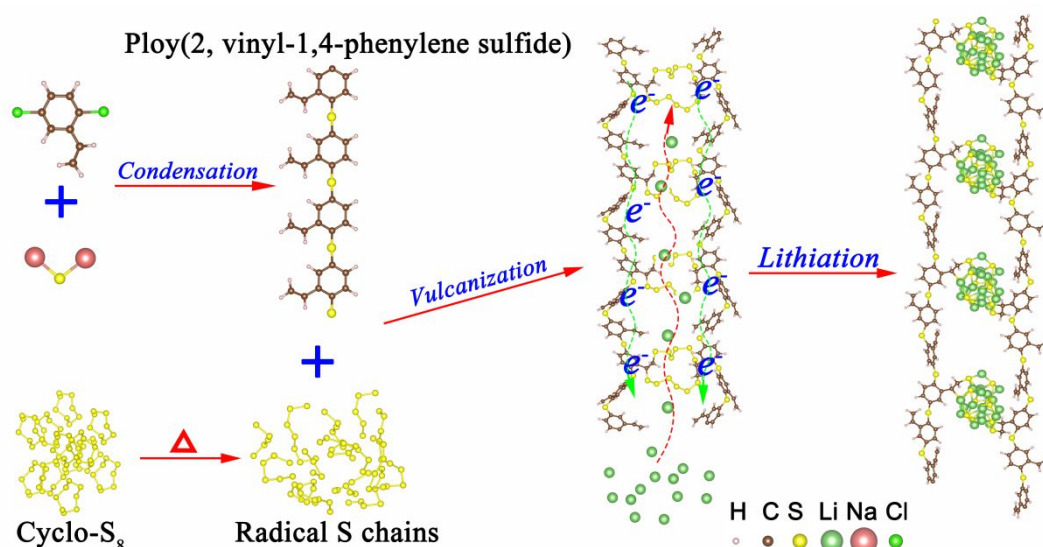
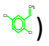
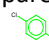
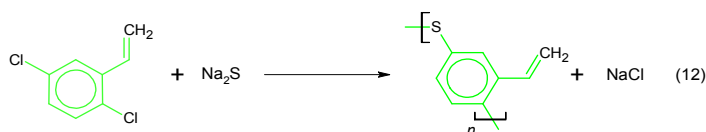


Figure 6 Schematic illustration of the preparation of Li-S cathode with poly (2-vinyl, 1, 4-phenylene sulfide)

Based on the above comparisons, we conclude that the crosslinking polymer is superior to the experimentally tested condensation polymer in terms of energy capacities, cycling stability, although both systems need to improve their electron conductivity. It is interesting to propose the Li-S cathode preparation process with poly (2-vinyl, 1, 4-phenylene sulfide) as shown in Fig. 6 based on theoretical investigation and experimental references²⁴. The monomer (2-vinyl, 1, 4-Dichlorobenzene, ) of the conductive poly (2-vinyl, 1, 4-phenylene sulfide) can be prepared by substituting one hydrogen on the benzene ring in the monomer (1, 4-Dichlorobenzene, ) of

poly (1, 4-phenylene sulfide) with vinyl. The poly (2-vinyl, 1, 4-phenylene sulfide) is formed by condensation of 2-vinyl, 1, 4-Dichlorobenzene with sodium sulfide, following the similar synthesis process of the poly (1, 4-phenylene sulfide):



The conductive property of this polymer can be enhanced by doping electron acceptor, like AsF_5 , in which the dopants induced defects in the conjugated backbone.³⁸ During the inverse vulcanization, cyclo- S_8 vaporizes and undergoes a thermal scission into radical sulfur chains at high temperature (above $185\text{ }^\circ\text{C}$)³⁹. Then, the poly (2-vinyl, 1, 4-phenylene sulfide) is added into orange molten sulfur via a syringe. The radical sulfur chains can be vulcanized onto the vinyl side chain of poly (2-vinyl, 1, 4-phenylene sulfide) via crosslinking addition reaction. During the lithiation process, the Li ions migrate into the S chain between poly (2-vinyl, 1, 4-phenylene sulfide) chains, meanwhile the electron transfer through the conductive backbone from the opposite direction. Since this material is also thermal-dynamic stable against Li_2S_n dissolution as discussed above, we thus believe the Li-S cathode system can be rather promising for practical applications.

Summary

In summary, we have proposed a practical approach to utilize the conduction materials, poly (2-vinyl, 1, 4-phenylene sulfide), via inverse vulcanization as a Li-S cathode. Such an approach is to address the issue of electron conductivity, low S content, and poor cycling stability in conventional polymer-based Li-S cathodes. Our theoretical investigation aims to address a few fundamental questions in such designs, including the limit of gravimetric and specific capacities; the structure stability; and electronic conductivity in the system. We found that: (1) The unsaturated C=C bonds in the edge is the most favorable sites for vulcanization via crosslinking; (2) substituting one hydrogen of poly (1, 4-phenylene sulfide) with the vinyl group for S vulcanization, has a limited influence on the electron conductivity of the backbone; (3) the most stable S chains for inverse vulcanization on the polymer are S_6^* ; (4) the S content obtained in our approach is extremely high: if 1/3 of the vinyl groups are vulcanized the S content is 49%, and the value can reach to 69% if all the vinyl groups are vulcanized. (5) During the lithiation process, the Li atoms break down the S-S bonds to forming Li_xS_t clusters gradually, while the strong covalent C-S bonds do not involve in the lithiation process, but confine the Li_xS_t clusters on the polymer. (6) these polymer cathodes exhibit a unique redox process with an average discharge voltage plateau of 1.51 V versus Li^+/Li , and the final discharge product has a formula of Li_2S ; (7) The maximum specific capacity and gravimetric energy densities for crosslinking polymers are 413 mAh/g and 626 Wh/kg, respectively (for fully vulcanized crosslinking configuration), which are much higher than the state-of-the-art Li-S value obtained by OXIS Energy Ltd(450 Wh/kg). (8) The positive dissolution energies throughout the whole discharge process, strong C-S covalent bond, and excellent kinetic stability in the electrolyte under ambient condition indicate the crosslinking polymer can restrict the shuttle effect efficiently in the whole discharge process, but it requires a small overpotential to activate it due to the small size; (9) The polymers are initially electron conductive through the band like charge transport.

However, as lithiation progresses, it becomes a Li-S cluster to Li-S cluster hopping transport. Future optimization might be necessary to make it maintain a backbone band structure transport for better conductivity. Overall, we believe the vulcanized conjugated polymer system can be a promising Li-S cathode system, better than the condensation ones tested so far experimentally. These studies will provide useful insights into the fundamental understanding of the polymer's roles in Li-S batteries and advanced cathode design for cheap and high-performance Li-S batteries.

Supporting information

The schematic of vulcanization S into Decene, the vulcanization energy of S into Decene, the DFT configures of vulcanization S into 5-Decene (a) and 1-Decene (b) via crosslinking, The Boltzmann distribution of different S chains during vulcanization at 185 °C, The configuration of Li_{11}S_6 on vulcanized polymer via condensation, the band structures with group velocities of valence band maximum (VBM or HOMO) and the conduction band minimum (CBM or LUMO) of the polymer via condensation after vulcanization (S_6^*), to lithiation ($\text{Li}_{10}\text{S}_6^*$), and the final structure of initial product vulcanization of S via crosslinking (a) and final lithiation production with $\text{Li}_{20}\text{S}_{12}$ on the poly (2-vinyl, 1, 4-phenylene sulfide) (b) within 1,2-dimethoxyethane(DME)/1,3-dioxolane(DOL) (mole ratio=1: 1) after *ab initio* molecular dynamics simulation in the NVT ensemble under 300 K with a time constant of 3000 fs.

Acknowledgment

This work was supported by the Assistant Secretary for Energy Efficiency and Renewal Energy of the U.S. Department of Energy under the Battery Materials Research (BMR) program. The theoretical work in this research used the resources of the NREL's high-performance computing (HPC) systems that are supported by the Office of Science of the U. S. Department of Energy.

Reference

1. S. Chu, Y. Cui and N. Liu, *Nat. Mater.*, 2017, 16, 16-22.
2. G. Zubi, R. Dufo-López, M. Carvalho and G. Pasaoglu, *Renew. Sustain. Energy Rev.*, 2018, 89, 292-308.
3. Z. W. Seh, Y. Sun, Q. Zhang and Y. Cui, *Chem. Soc. Rev.*, 2016, 45, 5605-5634.
4. G. Gao, F. Zheng and L.-W. Wang, *Chem. Mater.*, 2020, 32, 1974-1982.
5. G. Gao, F. Zheng, F. Pan and L.-W. Wang, *Adv. Energy Mater.*, 2018, 8, 1801823.
6. S. Huang, R. Guan, S. Wang, M. Xiao, D. Han, L. Sun and Y. Meng, *Prog. Polym. Sci.*, 2019, 89, 19-60.
7. M. J. Lacey, F. Jeschull, K. Edström and D. Brandell, *J. Phys. Chem. C*, 2014, 118, 25890-25898.
8. M.-K. Song, Y. Zhang and E. J. Cairns, *Nano Lett.*, 2013, 13, 5891-5899.
9. G. Li, M. Ling, Y. Ye, Z. Li, J. Guo, Y. Yao, J. Zhu, Z. Lin and S. Zhang, *Adv. Energy Mater.*, 2015, 5, 1500878.
10. H. Gao, Q. Lu, Y. Yao, X. Wang and F. Wang, *Electrochim. Acta*, 2017, 232, 414-421.
11. M. M. Doeff, M. M. Lerner, S. J. Visco and L. C. De Jonghe, *J. Electrochem. Soc.*, 1992, 139, 2077-2081.
12. B. Oschmann, J. Park, C. Kim, K. Char, Y.-E. Sung and R. Zentel, *Chem. Mater.*, 2015, 27, 7011-7017.

13. P. T. Dirlam, A. G. Simmonds, R. C. Shallcross, K. J. Arrington, W. J. Chung, J. J. Griebel, L. J. Hill, R. S. Glass, K. Char and J. Pyun, *ACS Macro Lett.*, 2015, 4, 111-114.
14. S. Zeng, L. Li, L. Xie, D. Zhao, N. Wang and S. Chen, *ChemSusChem*, 2017, 10, 3378-3386.
15. T. Nezakati, A. Seifalian, A. Tan and A. M. Seifalian, *Chem. Rev.*, 2018, 118, 6766-6843.
16. M. Wang, W. Wang, A. Wang, K. Yuan, L. Miao, X. Zhang, Y. Huang, Z. Yu and J. Qiu, *Chem. Commun.*, 2013, 49, 10263-10265.
17. L. E. Camacho-Forero and P. B. Balbuena, *Chem. Mater.*, 2020, 32, 360-373.
18. W. Jia, Z. Cao, L. Wang, J. Fu, X. Chi, W. Gao and L.-W. Wang, *Comput. Phys. Commun.*, 2013, 184, 9-18.
19. W. Jia, J. Fu, Z. Cao, L. Wang, X. Chi, W. Gao and L.-W. Wang, *J. Comput. Phys.*, 2013, 251, 102-115.
20. J. P. Perdew, K. Burke and M. Ernzerhof, *Phys. Rev. Lett.*, 1996, 77, 3865-3868.
21. J. P. Perdew, M. Ernzerhof and K. Burke, *J. Chem. Phys.*, 1996, 105, 9982-9985.
22. S. Grimme, *J. Comput. Chem.*, 2006, 27, 1787-1799.
23. J. George and N. V. Sastry, *Fluid Phase Equilib.*, 2004, 216, 307-321.
24. W. J. Chung, J. J. Griebel, E. T. Kim, H. Yoon, A. G. Simmonds, H. J. Ji, P. T. Dirlam, R. S. Glass, J. J. Wie, N. A. Nguyen, B. W. Guralnick, J. Park, Á. Somogyi, P. Theato, M. E. Mackay, Y.-E. Sung, K. Char and J. Pyun, *Nat. Chem.*, 2013, 5, 518-524.
25. A. G. Simmonds, J. J. Griebel, J. Park, K. R. Kim, W. J. Chung, V. P. Oleshko, J. Kim, E. T. Kim, R. S. Glass, C. L. Soles, Y.-E. Sung, K. Char and J. Pyun, *ACS Macro Lett.*, 2014, 3, 229-232.
26. P. Sang, Y. Si and Y. Fu, *Chem. Commun.*, 2019, 55, 4857-4860.
27. S. Perez Beltran and P. B. Balbuena, *J. Mater. Chem. A*, 2018, 6, 18084-18094.
28. S. Perez Beltran and P. B. Balbuena, *ChemSusChem*, 2018, 11, 1970-1980.
29. G. Zhou, A. Yang, G. Gao, X. Yu, J. Xu, C. Liu, Y. Ye, A. Pei, Y. Wu, Y. Peng, Y. Li, Z. Liang, K. Liu, L.-W. Wang and Y. Cui, *Sci. Adv.*, 2020, 6, eaay5098.
30. Z. Liu, H. Deng, W. Hu, F. Gao, S. Zhang, P. B. Balbuena and P. P. Mukherjee, *Phys. Chem. Chem. Phys.*, 2018, 20, 11713-11721.
31. J. Fanous, M. Wegner, J. Grimminger, Ä. Andresen and M. R. Buchmeiser, *Chem. Mater.*, 2011, 23, 5024-5028.
32. H. Hampson-Jones, Our cell and battery technology advantages, <https://oxisenergy.com/technology/>, Accessed 02/05/2020, 2020.
33. C.-W. Lee, Q. Pang, S. Ha, L. Cheng, S.-D. Han, K. R. Zavadil, K. G. Gallagher, L. F. Nazar and M. Balasubramanian, *ACS Cent. Sci.*, 2017, 3, 605-613.
34. L. Cheng, L. A. Curtiss, K. R. Zavadil, A. A. Gewirth, Y. Shao and K. G. Gallagher, *ACS Energy Lett.*, 2016, 1, 503-509.
35. A. Gupta, A. Bhargav and A. Manthiram, *Adv. Energy Mater.*, 2019, 9, 1803096.
36. Y. Zhao, C. Fang, G. Zhang, D. Hubble, A. Nallapaneni, C. Zhu, Z. Zhao, Z. Liu, J. Lau, Y. Fu and G. Liu, *Front. Chem.*, 2020, 8.
37. L. W. Shacklette, R. L. Elsenbaumer, R. R. Chance, H. Eckhardt, J. E. Frommer and R. H. Baughman, *J. Chem. Phys.*, 1981, 75, 1919-1927.
38. R. B. Dr Inamuddin, Mohammad Faraz Ahmer, Abdullah Mohamed Asiri, *Conducting polymers-based energy storage materials*, CRC Press,, Boca Raton, 2020.
39. B. Meyer, *Chem. Rev.*, 1976, 76, 367-388.